Structure of Mn-Si-Melts by Means of X-Ray Diffraction

E. Nassif*, P. Lamparter, B. Sedelmeyer, and S. Steeb

Max-Planck-Institut für Metallforschung, Institut für Werkstoffwissenschaften, Stuttgart

Z. Naturforsch. **38a**, 1093–1097 (1983); received June 16, 1983

The binary molten alloys $Mn_{74}Si_{26}$ and $Mn_{33.5}Si_{66.5}$ have been investigated by means of X-ray diffraction. The total structure factors as well as the total pair correlation functions were evaluated. The interatomic distances and total coordination numbers are given. The structural results for $Mn_{74}Si_{26}$ were compared to those for amorphous $Mn_{74}Si_{23}P_3$ and for a tetrahedral packing model. A pronounced shoulder on the second maximum of the structure factor, which normally is characteristic for the curves obtained with amorphous substances was observed for the $Mn_{74}Si_{26}$ melt. With the $Mn_{33.5}Si_{66.5}$ melt, however, this feature cold not be observed. Since with this concentration no glass forming by melt spinning is possible, a correlation between the shape of the second maximum of a total structure factor and the glass forming ability of the corresponding melt is suggested.

Introduction

In a previous study [1] structural data were obtained with the amorphous substance $Mn_{74}Si_{23}P_3$. In the present paper the structural relationship between the amorphous and the molten state is studied for the Mn-Si-system. This investigation is a continuation of corresponding experiments as were done with amorphous and molten Fe-B-alloys (see [2]).

Theoretical Basis

The total structure factor $S^{AL}(Q)$ is defined, following the Ashcroft-Langreth formulation [3] as

$$S^{AL}(Q) = I_{coh}/\langle f^2\rangle, \tag{1}$$

where

Q = $4\pi(\sin\theta)/\lambda$ = absolute value of the scattering vector $\boldsymbol{Q}$;
2θ = scattering angle;
λ = wavelength;
$\langle f^2\rangle = c_1 f_1^2(Q) + c_2 f_2^2(Q)$;
c_1, c_2 = molar fractions of the components 1, 2;
$f_1(Q), f_2(Q)$ = atomic scattering factors of the components 1, 2;
$I_{coh}(Q)$ = coherently scattered intensity per atom.

The coherently scattered intensity per atom $I_{coh}(Q)$ is obtained from the total measured intensity $I_T(Q)$ after being corrected for polarization [4], incoherent or Compton scattering [5], and normalized following the Krogh-Moe method [6]. The scattering factors were taken from [5] whereby atomic form factors for uncharged atoms were used. The Ashcroft-Langreth pair correlation function $G^{AL}(R)$ is obtained by Fourier transformation of $S^{AL}(Q)$:

$$G^{AL}(R) = \frac{2}{\pi}\int_0^{Q_m} Q\,[S^{AL}(Q) - 1]\sin(QR)\,\mathrm{d}Q \tag{2}$$

and can be expressed as follows:

$$G^{AL}(R) = 4\pi R\left[\varrho^{AL}(R) - \frac{\langle f\rangle^2}{\langle f^2\rangle}\varrho_0\right] \tag{3}$$

where $\varrho^{AL}(R)$ is the atomic density at a distance R from a reference atom, ϱ_0 the mean atomic number density and Q_m the maximum experimental Q-value.

The mean atomic number density ϱ_0 can be expressed as follows:

$$\varrho_0 = N_A\langle d\rangle/\langle A\rangle, \tag{4}$$

where $\langle d\rangle$ and $\langle A\rangle$ are the mean density and the mean atomic weight of he alloy, respectively, and where N_A is Avogadro's number.

* On leave of Departamento de Fisica, Facultad de Ingenieria, Universidad de Buenos Aires, Paseo Colon 850, 1063 Buenos Aires, Argentina.

Reprint requests to Prof. Dr. S. Steeb, Max-Planck-Institut für Metallforschung, Institut für Werkstoffwissenschaften, Seestraße, D-7000 Stuttgart.

0340-4811 / 83 / 1000-1093 $ 01.3 0/0. – Please order a reprint rather than making your own copy.

The coordination number N^{I} is calculated from the radial distribution function (RDF)

$$\mathrm{RDF}(R) = 4\pi R^2 \varrho^{\mathrm{AL}}(R)$$

according to

$$N^{\mathrm{I}} = \int_{R_{\mathrm{l}}}^{R_{\mathrm{u}}} \mathrm{RDF}(R)\, \mathrm{d}R, \tag{5}$$

where the lower and upper integration limits R_{l} and R_{u} refer to the minimum preceding and following the main peak of the RDF, respectively. $G^{\mathrm{AL}}(R)$ can be also expressed [7] in terms of the three partial pair correlation functions $G_{ij}(R)$ for a binary alloy:

$$G^{\mathrm{AL}}(R) = \frac{c_1^2 f_1^2}{\langle f^2 \rangle} G_{11}(R) + \frac{c_2^2 f_2^2}{\langle f^2 \rangle} G_{22}(R) + \frac{2 c_1 c_2 f_1 f_2}{\langle f^2 \rangle} G_{12}(R), \tag{6}$$

where $G_{ij}(R)$ represents the distribution of j-type atoms around an i-type atom. The $G_{ij}(R)$ are related to the corresponding partial distribution functions $\varrho_{ij}(R)$ as follows:

$$G_{ij}(R) = 4\pi R [\varrho_{ij}(R)/c_j - \varrho_0]. \tag{7}$$

Experimental

The measurements were performed in the reflection mode within a so called $\theta-\theta$ diffractometer in which the X-ray source and the scintillation detector move with the same angular speed while the free surface of the liquid sample remains horizontal. A primary graphite-monochromator was employed in order to produce monochromatic radiation from a 2 kW-molybdenum source ($\lambda_{\text{Mo-K}\alpha} = 0.71$ Å). All the measurements were done under 50 mbar gas pressure (Argon with 5 vol.% Hydrogen) to reduce manganese evaporation and to avoid manganese oxide layers on the sample surface.

By two diffraction experiments using a Tantalum sample once with and once without the protecting atmosphere, the correction of the experimental data for gas scattered background was done.

The cylindrical samples (50 mm diameter × 10 mm height) were heated on Boron-Nitrate crucibles within the high temperature chamber of the $\theta-\theta$-diffractometer up to 50 degrees above liquidus.

The total intensities I_{T} were recorded within $5° \leqq 2\theta \leqq 96°$ in time preset mode using variable step widths between 0.3° and 0.9° in 2θ. The resolution power was about $\Delta 2\theta = 0.5°$ in the range of the main peak which is sufficient for diffraction studies on molten alloys. The relative statistical error for the measured points in each was better than 1.5%.

Controlling of the experiments and data collection was done by a computer (DEC-PDP 11-03L) via a telecomputer-interface. For further evaluation the data were transferred to a central computer. In order to recognize possible modifications of the condition of the melt and condensation of metal vapours onto the windows of the chamber for each measurement four or five scans were performed each of them lasting about one hour. Making sure that no significant changes had taken place in the different scans all data were superposed before further evaluation work was done.

Results and Discussion

I. Molten Mn-Si Containing 26 at.% Si

a) Structure Factor

In Fig. 1 the Ashcroft-Langreth structure factor $S^{\mathrm{AL}}(Q)$ for molten $Mn_{74}Si_{26}$ is compared with that of amorphous $Mn_{74}Si_{23}P_3$ [1] and with that of the $Mn_{33.5}Si_{66.5}$ melt. More pronounced oscilla-

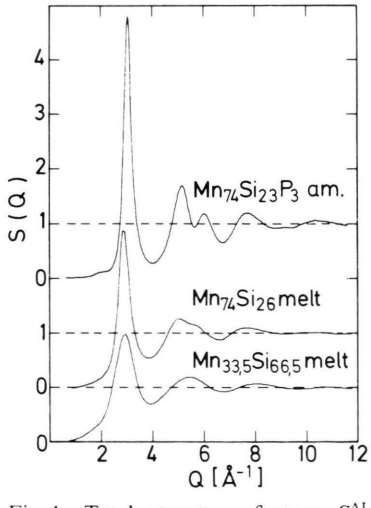

Fig. 1. Total structure factors $S^{\mathrm{AL}}(Q)$ measured with Mo-Kα-radiation for amorphous $Mn_{74}Si_{23}P_3$ (see [1]), molten $Mn_{74}Si_{26}$, and molten $Mn_{33.5}Si_{66.5}$.

tions can be observed for the structure factor in the amorphous case compared to that of the liquid state. It can also be seen that the main peak of the structure factor curve for the $Mn_{74}Si_{26}$ liquid alloy is located at an essentially lower Q-value compared to that of the amorphous case.

The most important feature, however, is the appearance of a pronounced shoulder on the second maximum of the structure factor of molten $Mn_{74}Si_{26}$. This shoulder, characteristic for amorphous alloys and here partially preserved in the liquid state has been up to now only observed in molten alloys of the iron-boron system [2]. In the same way as already mentioned above for the main maximum of the structure factor also the second maximum of the structure factor of the melt as well as the shoulder shows up a displacement to lower Q-values compared to the position of the corresponding maxima of the structure factor of the $Mn_{74}Si_{23}P_3$ amorphous alloys.

A further difference between the structure factor in Fig. 1 of the amorphous alloy and that of the molten alloy containing 26 at.% Si can be observed at $Q \cong 2\,\text{Å}^{-1}$. At this position the structure factor obtained with the amorphous alloy shows a pre-maximum which is not present in the curve obtained with the molten alloy.

Finally, attention should be drawn to the differences in the half width ΔQ of the two main maxima obtained with the alloys containing 74% Mn. ΔQ amounts to $0.57\,\text{Å}^{-1}$ in the molten case and to $0.42\,\text{Å}^{-1}$ in the case of the amorphous alloy. Corresponding to the relation $\xi = 2\pi/\Delta Q$ these half widths yield the correlation lengths $\xi = 11$ Å and 15 Å, respectively.

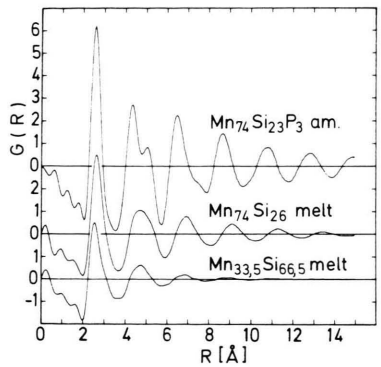

Fig. 2. Total pair correlation functions $G^{AL}(R)$ calculated from the $S^{AL}(Q)$-curves in Fig. 1 for amorphous $Mn_{74}Si_{23}P_3$ (see [1]), molten $Mn_{74}Si_{26}$, and molten $Mn_{33.5}Si_{66.5}$.

b) Pair Correlation Function and Coordination Number

From the Ashcroft-Langreth structure factors $S^{AL}(Q)$, the corresponding total pair correlation functions for amorphous $Mn_{74}Si_{23}P_3$ and for the $Mn_{74}Si_{26}$- as well as the $Mn_{33.5}Si_{66.5}$-melt were calculated following Eq. (2) and plotted in Figure 2. The main peak as well as the second and further maxima of the $G^{AL}(R)$-curve for the liquid $Mn_{74}Si_{26}$ alloy are shifted to higher R-values compared to the data of the amorphous alloy as can be well seen on Table 1. It can be seen that the first partial maximum

Table 1. T = temperature of the melt, ϱ_0 = atomic density, N^I, R^I = total coordination number and atomic distance, respectively, for the first shell of the total pair correlation function, R_1^{II}, R_2^{II}, R^{III} = further atomic distances, calculated from the total pair correlation function (subindex indicates first and second partial maxima, respectively, of the second peak). R_2^{II} for the melt containing 26 at.% Si was taken as the position of the shoulder.

	T (°C)	ϱ_0 $\left(\frac{\text{Atoms}}{(\text{Å})^3}\right)$	N^I	R^I (Å)	R_1^{II} (Å)	R_2^{II} (Å)	R^{III} (Å)	$\frac{R_1^{II}}{R^I}$	$\frac{R_2^{II}}{R^I}$	$\frac{R^{III}}{R^I}$
$Mn_{74}Si_{23}P_3$ [1] (amorphous)	–	0.0688	11.6	2.60	4.35	5.05	6.46	1.67	1.94	2.48
$Mn_{74}Si_{26}$-melt	1180	0.0600	11.2	2.65	4.76	5.25	6.95	1.80	1.98	2.62
$Mn_{33.5}Si_{66.5}$-melt	1170	0.0565	9.2	2.55	4.76	–	6.85	1.87	–	2.69
Model following Wright [8]	–	–	–	–	–	–	–	1.67	2.00	2.52
Model following Takeuchi [9]	–	–	–	–	–	–	–	1.65	1.93	2.52

of the second peak of the $G^{AL}(R)$-curve which is rather pronounced for the amorphous alloy, almost disappears for the molten alloy and only a slight asymmetry is still observed. In Table 1 also the normalized atomic distances are listed for molten $Mn_{74}Si_{26}$ and amorphous $Mn_{74}Si_{23}P_3$ as well as those obtained from tetrahedral models [8], [9].

Whereas the data for the amorphous alloy show rather good agreement with those of the tetrahedral model, larger values of the normalized atomic distances for the $Mn_{74}Si_{26}$ molten alloy are obtained. This feature and the broadening of the main peak of the structure factor for the liquid specimen can be interpreted as an evidence for a more disordered atomic structure in the melt. It must be remarked, however, that the $Mn_{74}Si_{26}$-melt shows rather extended topologial ordering compared to other melts. Perhaps the indication of a shoulder on the right hand side of the second maximum of the $G^{AL}(R)$-curve of the molten Mn-Si alloy containing 26 at.% Si can be interpreted as caused by a smeared out tetrahedral arrangement which in its more perfect form yields a double maximum as shown in the $G^{AL}(R)$-curve of the amorphous alloy.

According to Eq. (6), the Ashcroft-Langreth total pair correlation function can be expressed in terms of the partial correlation functions as follows:

$$G^{AL}(R) = 0.667\, G_{MnMn} + 0.026\, G_{SiSi} + 0.262\, G_{MnSi}. \quad (8)$$

This equation shows that the run of the total $G^{AL}(R)$ is mainly determined by the Mn-Mn-pairs and in a less pronounced manner by the Mn-Si-pairs.

The atomic distances obtained from the measured data for the first neighbourhood amount to 2.60 Å for amorphous $Mn_{74}Si_{23}P_3$ and to 2.65 Å for the $Mn_{74}Si_{26}$ molten alloy and thus are in good agreement with the diameter 2.70 Å of the Mn atoms as taken from [10].

The total coordination numbers taken from the total pair correlation function following Eq. (5) are listed up in Table 1 and are almost equal for the amorphous (11.2) and the liquid alloys (11.6).

II. Molten Mn-Si Containing 66.5 at.% Si

a) Structure Factor

The Ashcroft-Langreth structure factor $S^{AL}(Q)$ for the $Mn_{33.5}Si_{66.5}$ molten alloy is plotted in Figure 1.

The main maximum lies at a larger Q-value for the melt with larger Si-content which can be understood regarding the smaller diameter of the Si-atoms compared to that of the Mn-atoms.

The height of the main peak decreases with larger Si-content which means a softening of the atomic arrangement.

The comparison of the correlation lengths as obtained from the half widths of the main peaks yields 6 Å for the $Mn_{33.5}Si_{66.5}$ melt and 11 Å for molten $Mn_{74}Si_{26}$. It can be observed that there is no shoulder on the right hand side of the second maximum of the structure factor curve. Thus this melt behaves similar to nearly all melts studied up to now with the exception of Fe-B-melts [2] and the $Mn_{74}Si_{26}$-melt of Figure 1.

Finally, attention should be drawn to the larger period of $S^{AL}(Q)$ for the melt with larger Si-content.

b) Pair Correlation Function and Coordination Number

The pair correlation function for the $Mn_{33.5}Si_{66.5}$-melt is shown in Figure 2. For this composition the $G^{AL}(R)$-function can be expressed in terms of the partial correlation functions as follows:

$$G^{AL}(R) = 0.206\, G_{MnMn} + 0.255\, G_{SiSi} + 0.459\, G_{MnSi}. \quad (9)$$

In this case, the contribution G_{MnSi} of the mixed correlations is stronger weighted than the contribution G_{MnMn}. If one takes for the diameters d of both components the values

$$d_{Mn} = 2.70 \text{ Å} \quad \text{and} \quad d_{Si} = 2.34 \text{ Å} \quad \text{(see [1])},$$

the distance between Mn- and Si-atoms should be $d_{Mn\text{-}Si} = 2.52$ Å. From the values d_{Mn} and $d_{Mn\text{-}Si}$ and keeping in mind the weighting factors of (8) and (9) one can explain the position of the main maximum of the $Mn_{33.5}Si_{66.5}$-melt compared to the corresponding position within the $Mn_{74}Si_{26}$-curve (see Table 1).

A further difference between the curves of the two molten alloys is the strong damping of the oscillations which corresponds to the shorter correlation length obtained for this composition from the half width of the first maximum of the structure factor. The coordination number for the $Mn_{33.5}Si_{66.5}$-melt amounts to $N^I = 9.5$.

The normalized atomic distances as shown in Table 1 show a rather large discrepancy compared

to those of Wright's tetrahedral-model. Melts containing 66.5 at.% Si cannot be quenched into the amorphous state by melt spinning. Thus our working hypothesis that there is a connection between the splitting up of the second maximum of the structure factor and of the pair correlation function and the glass forming ability of a melt is supported.

Summary

The atomic structure of the molten alloys $Mn_{74}Si_{26}$ and $Mn_{33.5}Si_{66.5}$ has been investigated by means of X-ray diffraction experiments. The experimental results were compared with those obtained for amorphous $Mn_{74}Si_{23}P_3$. For the $Mn_{74}Si_{26}$-melt characteristic features of the amorphous alloy at almost the same concentration, such as a pronounced shoulder on the second maximum of the structure factor and a rather extended topological correlation were found.

The $Mn_{33.5}Si_{66.5}$ molten alloy, which does not fall in the glass forming composition range of this system, shows no shoulder and a rather restricted extension of the topological correlations. These are typical attributes to almost all the liquid systems studied up to now with the exception of $Mn_{74}Si_{26}$ from the present work and two melts of the Fe-B-system, all three of them being glass formers.

The normalized atomic distances were taken from the total pair correlation functions for the $Mn_{74}Si_{26}$- as well as the $Mn_{33.5}Si_{66.5}$-melt and have been compared with those obtained for a tetrahedral model. The agreement between this model and the latter melt is rather poor, however, the $Mn_{74}Si_{26}$-melt seems to represent a smeared out tetrahedral arrangement.

Acknowledgements

Thanks are due to the Deutsche Forschungsgemeinschaft (DFG), Bad Godesberg, for financial support of this work.

[1] G. Rainer-Harbach, P. Lamparter, F. Paasche, and S. Steeb, Proc. 4th Int. Conf. on Rapidly Quenched Metals (RQ4), Sendai (1981), Vol. 1, p. 315.
[2] E. Nold, G. Rainer-Harbach, P. Lamparter, and S. Steeb, Z. Naturforsch. **38a,** 325 (1983).
[3] N. W. Ashcroft and D. C. Langreth, Phys. Rev. **156,** 685 (1967).
[4] R. W. James, The Optical Principle of the Diffraction of X-Rays, G. Bell and Sons Ltd., London 1958.
[5] J. H. Hubbell et al., J. Phys. Chem. Ref. Data Vol. **4,** No. 3, 471 (1975).
[6] J. Krogh-Moe, Acta Cryst. **9,** 951 (1956).
[7] C. N. J. Wagner, J. Non Cryst. Sol. **31,** 1 (1978).
[8] J. G. Wright, Phil. Mag. **30,** 995 (1974).
[9] S. Takeuchi, S. Kobayashi, Phys. Stat. Sol. (a) **65,** 315 (1981).
[10] W. Hume Rothery and G. V. Raynor, The Structure of Metals and Alloys, Inst. Metals, London 1954.